

Nhanes 2022 Blood Pressure-Based Mortality Risk - Appendix A

Rscripts by Hamish Patten, DW Bester and David Steinsaltz

23/12/2022

Contents

Appendix A - Further Detail on Modelling and Results	1
Model	1
Survival Analysis (Time-to-Event)	2
Longitudinal Modelling	3
Combined Hierarchical Model	4
The modelling variants	4
Methodology	5
Empirical Bayes Parameters	7
Extract intervals for the digits	7
Fit the BP distribution parameters	7
Now compute the combined variance	9
Computing residuals	9
Check variance distribution empirically	10
Hamiltonian Monte Carlo (HMC)	12
Centering the Linear Predictor	13
Code Description	13
Data Cleaning	13
Main	13
Stan	14
Centering	14
Empirical Bayes Estimation	14
Results	14
Convergence of Simulations	14
Results - Model Parameterization	17

Appendix A - Further Detail on Modelling and Results

This appendix aims to add more detail about the numerical modelling than was provided in the article. This is to ensure that the research methods are transparent and entirely reproducible. The numerical modelling presented in this paper was performed using R combined with Rstan. More detail will be provided here about the model, about the specific methodology used to parameterize the model, and more results are provided that were not included in the main bulk of the article.

Model

The model used in this research is built from the theory of joint modelling of longitudinal and time-to-event data. This will be described in detail later on in this section, however, in brief, this allows the simultaneous

modelling of both longitudinal observation data (in this article, this is blood pressure measurements) and also the time-to-event outcome. In this research the event of interest is either death from any cause, or death from specifically cardiovascular or cerebrovascular disease (CVD). In the latter case death from a different cause is treated as a noninformative censoring event.

Survival Analysis (Time-to-Event)

The basic survival model is a Gompertz hazard rate with proportional hazards influences of the blood pressure covariates. The Gompertz equation

$$h_0(t) = B \exp(\theta(x + T)), \quad (1)$$

describes the baseline hazard of the population to a particular risk, which, for this article, investigates CVD mortality specifically, as well as studying mortality risk in general. $x \in \mathbb{N}^{\mathbb{N}}$ is the age of the individual at the initial interview time, for N the number of individuals, and $T \in \mathbb{R}^{+,N}$ the time since the individual entered the survey. Note that both B and θ have 6 different values, depending on the sex reported at the initial interview – female or male — or the race — black, white or ‘other’. Note that ‘other’ in the race category is a combination of all non-black or non-white racial identities, such as Hispanic populations. The log-linear proportional hazards model links the covariates of the model (mean systolic blood pressure, variance in the diastolic blood pressure, etc) to the survival outcome of the individual via the equation

$$h(t) = h_0(t) \exp(\beta \cdot (\mathbf{X} - \hat{\mathbf{X}})), \quad (2)$$

where $\mathbf{X} \in \mathbb{R}^{+,N \times d}$ is a vector of summary statistics of the blood pressure measurements of individual covariates in our model, $\hat{\mathbf{X}} \in \mathbb{R}^{+,d}$ is the centering of the covariates such that the equation $\sum_i^N \exp(\beta \cdot (\mathbf{X} - \hat{\mathbf{X}})) = 0$ is approximately satisfied (more on this later), and $\beta \in \mathbb{R}^d$ implies the strength of the influence of the covariate on the mortality risk. The majority of mortality events are censored — not yet known at the time of data collection — the censoring indicator being notated as $\delta \in \{0, 1\}$. When CVD mortality is the event being analysed, deaths due to other causes are treated as noninformative censoring events. In this study, we explored the following covariates:

Variable Name	Support	Description
$FRS - 1998$	R^N	1998 version of the FRS score
$FRS - ATP$	R^N	ATP version of the FRS score
M_S	$R^{+,N}$	Mean systolic blood pressure
M_D	$R^{+,N}$	Mean diastolic blood pressure
Δ_S	$R^{+,N}$	Difference between Home and Clinic mean systolic blood pressure
Δ_D	$R^{+,N}$	Difference between Home and Clinic mean diastolic blood pressure
$\sigma_{\{S,H\}}$	$R^{+,N}$	Standard deviation of the systolic blood pressure taken at home
$\sigma_{\{D,H\}}$	$R^{+,N}$	Standard deviation of the diastolic blood pressure taken at home
$\sigma_{\{S,C\}}$	$R^{+,N}$	Standard deviation of the systolic blood pressure taken at the clinic
$\sigma_{\{D,C\}}$	$R^{+,N}$	Standard deviation of the diastolic blood pressure taken at the clinic
$\tau_{\{S,H\}}$	$R^{+,N}$	Precision of the systolic blood pressure taken at home
$\tau_{\{D,H\}}$	$R^{+,N}$	Precision of the diastolic blood pressure taken at home
$\tau_{\{S,C\}}$	$R^{+,N}$	Precision of the systolic blood pressure taken at the clinic
$\tau_{\{D,C\}}$	$R^{+,N}$	Precision of the diastolic blood pressure taken at the clinic

Please note that the last four elements of this list, the precision values, were only carried out to ensure model consistency with the use of standard deviation instead. Note as well that the Δ covariates, representing the medium-term variability, enter into the log relative risk sum as an **absolute value**.

For the parametrization of this model, we assume that the Gompertz parameters and the parameters in the

linear predictor term are distributed as follows:

$$\begin{aligned} \mathbf{B} &\sim \mathbb{C}(\mu_B, \sigma_B), \\ \boldsymbol{\theta} &\sim \mathfrak{N}(\mu_\theta, \sigma_\theta), \\ \boldsymbol{\beta} &\sim \mathfrak{N}(\mu_\beta, \sigma_\beta), \end{aligned} \tag{3}$$

noting that $\mathbb{C}(\mu, \sigma)$ is the Cauchy distribution.

The likelihood for this Gompertz proportional hazards model, over all individuals in the census, is as follows:

$$L_S(\mathbf{v}, \boldsymbol{\delta}) = \prod_i^N f(v_i, \delta_i | B_i, \theta_i, \beta_i, \mathbf{X}, \hat{\mathbf{X}}) = \prod_i^N h(v_i | B_i, \theta_i, \beta_i, \mathbf{X}, \hat{\mathbf{X}})^{\delta_i} \exp \left(- \sum_i^N H(v_i | B_i, \theta_i, \beta_i, \mathbf{X}, \hat{\mathbf{X}}) \right), \tag{4}$$

with $H(v) = \int_0^v h(w)dw$ the cumulative hazard.

Longitudinal Modelling

The mortality hazard rates are assumed to be influenced by individual-level blood pressure means and variability characteristics. These characteristics are not directly observed, but are inferred from their influence on the individual blood pressure measurements, which have been observed. Let $Y_i(t_j)$ be the observed blood pressure for patient i at time t_j , for the individual $i \in 1, 2, \dots, N$ and the number of blood pressure measurements per individual $j \in 1, 2, \dots, k$. Due to the fact that the blood pressure measurement data was taken at both the home and clinic (written using subscripts H and C, respectively), with approximately 6 months between these two measurements, we model the blood pressure using the following model, assuming the diastolic Y_i^D and systolic Y_i^S blood pressure to be Gaussian-distributed:

$$\begin{aligned} (Y_i^D)_H &\sim \mathfrak{N}(M_i^D + \Delta_i^D, (\sigma_i^D)_H), \\ (Y_i^D)_C &\sim \mathfrak{N}(M_i^D - \Delta_i^D, (\sigma_i^D)_C), \\ (Y_i^S)_H &\sim \mathfrak{N}(M_i^S + \Delta_i^S, (\sigma_i^S)_H), \\ (Y_i^S)_C &\sim \mathfrak{N}(M_i^S - \Delta_i^S, (\sigma_i^S)_C), \end{aligned} \tag{5}$$

where superscripts D and S refer to diastolic and systolic blood pressure, respectively.

The blood pressure characteristics — the individual-level parameters — are themselves distributed according to a hierarchical model, determined by population-level parameters (also called “hyperparameters”):

$$\begin{aligned} M_i^{\{D,S\}} &\sim \mathfrak{N}(\mu_M^{\{D,S\}}, \sigma_M^{\{D,S\}}), \\ \Delta_i^{\{D,S\}} &\sim \mathfrak{N}(\mu_D^{\{D,S\}}, \sigma_D^{\{D,S\}}), \\ \sigma_{i,C}^{\{D,S\}} &\sim \Gamma(r_C^{\{D,S\}}, \lambda_C^{\{D,S\}}), \\ \sigma_{i,H}^{\{D,S\}} &\sim \Gamma(r_H^{\{D,S\}}, \lambda_H^{\{D,S\}}). \end{aligned} \tag{6}$$

The longitudinal outcome modelling therefore aims to infer these hyperparameters

$$\Theta = \left\{ \mu_M^{\{D,S\}}, \mu_D^{\{D,S\}}, \sigma_M^{\{D,S\}}, \sigma_D^{\{D,S\}}, r_C^{\{D,S\}}, \lambda_C^{\{D,S\}}, r_H^{\{D,S\}}, \lambda_H^{\{D,S\}} \right\}, \tag{7}$$

and to use the implied uncertainty about the individual-level parameters to inform the inference about the survival parameters. The likelihood for the longitudinal measurements is therefore (combining the systolic and diastolic into a single parameter for simplicity):

$$L_L(\Theta | Y) = \prod_{i=1}^N \left(\prod_{j=1}^k f(y_{ij} | M_i, \Delta_i, \sigma_i) \right) f(M_i | \mu_M, \sigma_M) f(\Delta_i | \mu_D, \sigma_D) f(\tau_{i,C} | r_C, \lambda_C) f(\tau_{i,H} | r_H, \lambda_H) \tag{8}$$

Combined Hierarchical Model

Combining the longitudinal outcome and time-to-event partial likelihoods, and for a given parameter space value of $\Omega = \{\beta, B, \theta\} \cup \Theta$, the joint likelihood is

$$L(\Omega|Y) = \prod_{i=1}^N \left(\prod_{j=1}^k f(y_{ij}|M_i, \Delta_i, \sigma_i) \right) f(v_i, \delta_i|B_i, \theta_i, \beta_i, \mathbf{X}, \hat{\mathbf{X}}) f(M_i|\mu_M, \sigma_M) f(\Delta_i|\mu_D, \sigma_D) f(\tau_{i,C}|r_C, \lambda_C) f(\tau_{i,H}|r_H, \lambda_H). \quad (9)$$

One approach to estimating the complete set of hyperparameters

$$\Omega_H = \{\mu_B, \sigma_B, \mu_\theta, \sigma_\theta, \mu_\beta, \sigma_\beta, \mu_M^{\{D,S\}}, \sigma_M^{\{D,S\}}, \mu_D^{\{D,S\}}, \sigma_D^{\{D,S\}}, r_C^{\{D,S\}}, \lambda_C^{\{D,S\}}, r_H^{\{D,S\}}, \lambda_H^{\{D,S\}}\} \quad (10)$$

is to impose a higher-level prior distribution, and use the machinery of Bayesian inference to produce posteriors for everything. This approach runs into computational difficulties, which have led us to a two-stage “empirical Bayes” approach, where the hyperparameters for the longitudinal model are first fixed by a maximum-likelihood calculation, after which the remaining hyperparameters and individual-level parameters can be estimated with Bayesian machinery. For the time-to-event parameters we choose flat hyperpriors, selecting the hyperparameters $\mu_B = \mu_\theta = \mu_\beta = 0$, $\sigma_B = \sigma_\theta = 2$, and $\sigma_\beta = 100$.

The modelling variants

In this article, we researched into 16 variants of the model-fitting problem, but focussed mainly on 8 of them. The 8 main models use the standard deviation, σ , as the measure of the influence of blood-pressure variability on mortality. We also produced the same 8 models but using precision, $\tau = 1/\sigma^2$, as the measure of the influence of blood-pressure variability on mortality. However, this was only to ensure that there were no differences between the use of one over the other. Throughout the remainder of this appendix, we refer to the 8 main models using the following run numbers:

1. All participants (15,295), using mean systolic and diastolic blood pressure (not FRS) in the linear predictor term, with the outcome data as death specifically from CVD.
2. All participants (15,295), using mean systolic and diastolic blood pressure (not FRS) in the linear predictor term, with the outcome data as all-causes of death.
3. Only participants that had data from which FRS values could be computed (N=9,418) — the “FRS population” but using mean systolic and diastolic blood pressure (not FRS) in the linear predictor term, with the outcome data as death specifically from CVD.
4. FRS population, but using mean systolic and diastolic blood pressure (not FRS) in the linear predictor term, with the outcome data as all-causes of death.
5. FRS population, and using the FRS ATP-III value in the linear predictor term, with the outcome data as death specifically from CVD.
6. FRS population, and using the FRS ATP-III value in the linear predictor term, with the outcome data as all-causes of death.
7. FRS population, and using the FRS 1998-version value in the linear predictor term, with the outcome data as death specifically from CVD.
8. FRS population, and using the FRS 1998-version value in the linear predictor term, with the outcome data as all-causes of death.

We also include Directed Acyclical Graph (DAG) sketches to help visualize the different models, as shown in figures 1 and 2. In order to read the DAGs, note that each square background layer that appears as a stack of layers represents different measured outcomes that were made in the first wave of the survey. The

outcome variables measured are represented by a square-shaped text box, and a parameter of the model is represented by a circular-shaped text box. If either a square or circular text box is placed on top of a stacked rectangular layer, it means that multiple values of that variable (as many as there are layers to the stack) are either measured (for outcome variables) or simulated (for parameters of the model). Please note that the number of layers in the stack is written in the text box that does not contain a frame which is intentionally displayed on top of the stacked layer that it represents. For example, $i = 1, \dots, N$. Finally, the direction of the arrows implies causality assumed in the model.

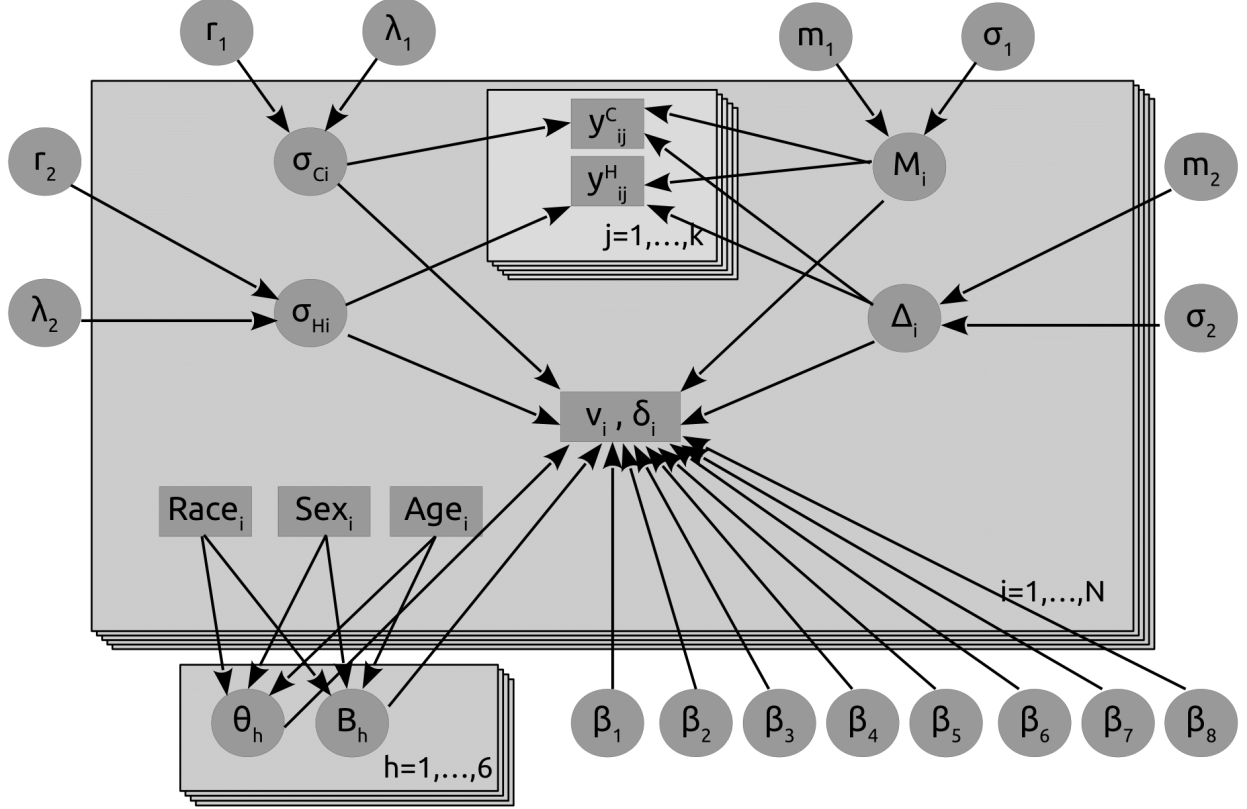


Figure 1: An illustration of the DAG of the mean blood pressure-based model presented in this article.

Methodology

The methodology for this research can be split into three main sections: 1) calculating the empirical Bayes' parameters, 2) parameterizing the model using Hamiltonian Monte Carlo (HMC) and 3) re-centering the variables in the linear predictor equation. By applying empirical Bayes', Maximum Likelihood Estimates (MLEs) of some of the parameter distributions are provided. Note that the parameters estimated here are only the prior distribution of the global (not individual) blood pressure means and the variances, for both systolic and diastolic and home and clinic measurements. These estimates are then provided as prior distributions for the Stan MCMC simulations using HMC, where estimates can be made for all the parameter distributions of the model, given the specific centering applied. Finally, section (3) recalculates the centering values based on the previous MCMC iteration, and sets of the next iteration, while simultaneously checking for convergence in both the MCMC simulations and the centering values.

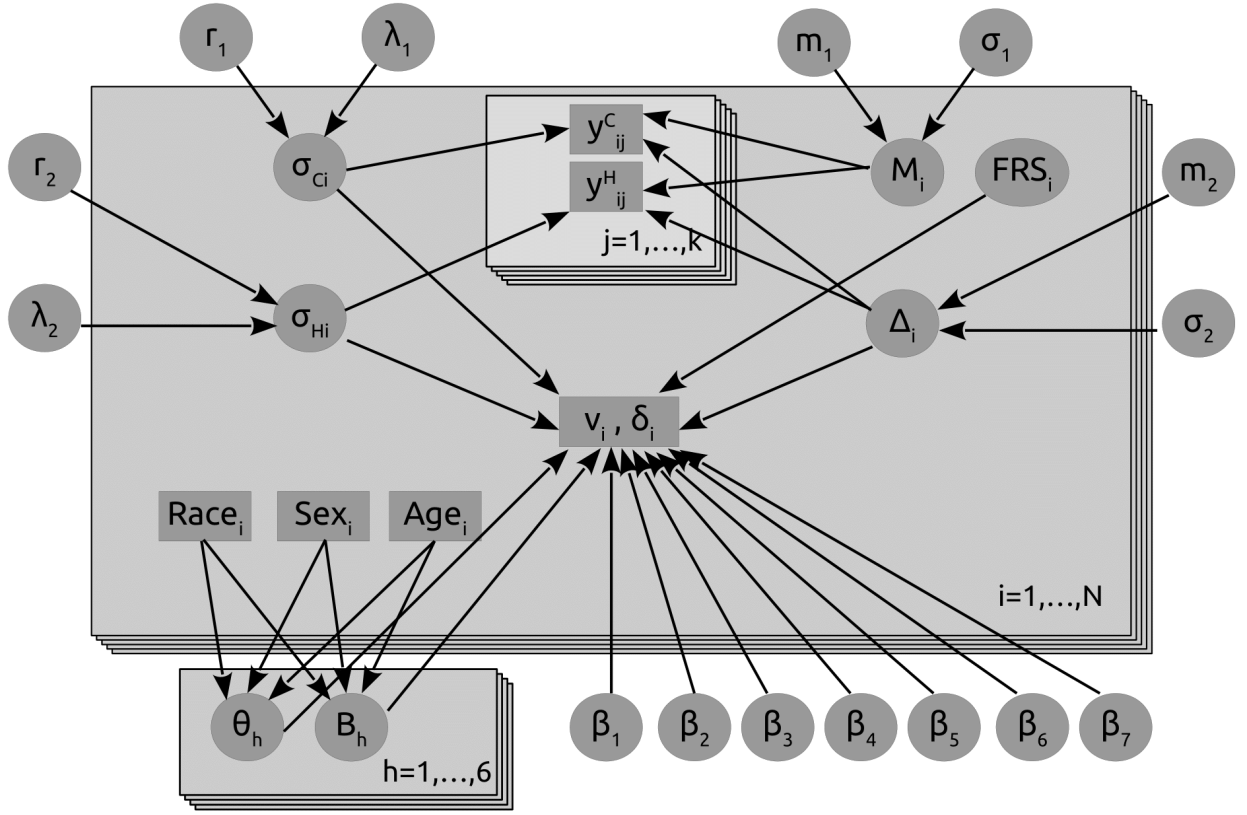


Figure 2: An illustration of the DAG of the FRS-based model presented in this article.

Empirical Bayes Parameters

Extract intervals for the digits

Suppose the fractions of digits 0,2,4,6,8 are b_0, b_2, b_4, b_6, b_8 . Letting $B_0 = 0$ and $B_k = 10 \sum_{j=0}^{k-1} b_{2j}$ for $k = 1, \dots, 5$, we want to choose a positive a and place breaks at $-a + B_k$, so that measurements between $-a + B_k$ and $-a + B_{k+1}$ modulo 10 are assigned the final digit $2k$, for $k = 0, \dots, 4$. We choose a to minimise the total distance of the intervals from the rounded value:

$$\sum_{k=0}^4 \int_{-a+B_k}^{-a+B_{k+1}} |x - 2k| dx = \frac{1}{2} \sum_{k=0}^4 (-a + B_k - 2k)^2 + (-a + B_{k+1} - 2k)^2,$$

as long as $2k$ is in the appropriate interval. This is minimized at

$$a = \frac{1}{5} (B_1 + B_2 + B_3 + B_4 - 15) = \sum_{j=0}^3 (8 - 2j) b_{2j} - 3.$$

Fit the BP distribution parameters

We suppose that each individual has BP measures \tilde{y}_{ij}^l for $i = 1, \dots, n$, $j = 1, \dots, k$ (default $k = 3$), and $l = 1, 2$, which are rounded versions of

$$y_{ij}^l \sim \mathcal{N}(\mu_i^l, (\tau_i^l)^{-1}),$$

where

$$\begin{aligned} \mu_i^1 &= (M_i + \Delta_i)/2, \\ \mu_i^2 &= (M_i - \Delta_i)/2, \\ M_i &\sim \mathcal{N}(m_M, \sigma_M^2) \text{ and } \Delta_i \sim \mathcal{N}(m_\Delta, \sigma_\Delta^2) \text{ independent,} \\ \tau_i^l &\sim \text{Gamma}(\alpha^l, \alpha^l/\theta^l). \end{aligned}$$

(Note that α^l is the usual shape parameter, while θ^l is the expectation.)

We wish to estimate the eight parameters

$$(m_M, m_\Delta, \sigma_M^2, \sigma_\Delta^2, \alpha^1, \theta^1, \alpha^2, \theta^2)$$

We begin by assuming y_{ij}^l observed directly. We estimate by maximising the partial likelihood on the observations

$$\begin{aligned} \bar{y}_{i+} &:= \frac{1}{2k} \sum_{j=1}^k y_{ij}^1 + y_{ij}^2, \\ \bar{y}_{i-} &:= \frac{1}{2k} \sum_{j=1}^k y_{ij}^1 - y_{ij}^2, \\ s_i^l &:= \frac{1}{k-1} \sum_{j=1}^k \left(y_{ij}^l - \frac{1}{k} \sum_{j=1}^k y_{ij}^l \right)^2. \end{aligned}$$

Note that

$$(k-1)s_i^l \tau_i^l = \sum_{j=1}^k \left(z_{ij}^l - \frac{1}{k} \sum_{j=1}^k z_{ij}^l \right)^2.$$

where z_{ij}^l are i.i.d. standard normal is independent of τ_i^l , thus has a chi-squared distribution with $k-1$ degrees of freedom — hence $\frac{k-1}{2} \cdot s_i^l \tau_i^l$ is gamma distributed with parameters $(\frac{k-1}{2}, 1)$. Since $\frac{\alpha}{\theta} \tau_i^l$ is independent of

$s_i^l \tau_i^l$, with $\text{Gamma}(\alpha, 1)$ distribution, we see that $\frac{\theta(k-1)}{2\alpha} s_i^l$ is the ratio of two independent gamma random variables, hence has beta-prime distribution with parameters $(\frac{k-1}{2}, \alpha)$, so log partial likelihood

$$\ell_{\text{Beta}}(\alpha, \theta; s^l) = n\alpha \log \frac{\alpha}{\theta} + n \log \Gamma\left(\alpha + \frac{k-1}{2}\right) - n \log \Gamma(\alpha) + \frac{k-1}{2} \sum_{i=1}^n \log s_i^l - \left(\alpha + \frac{k-1}{2}\right) \sum_{i=1}^n \log\left(s_i^l + \frac{\alpha}{\theta}\right).$$

Note as well that these quantities $(k-1)s_i^l$ should correspond to empirically observed individual variances; hence we will compare these empirical variances (with imputed fractional parts) divided by the normalization factor $2\alpha/(k-1)\theta$ to the beta-prime distribution below as a goodness-of-fit test.

The partial Fisher Information has entries

$$\begin{aligned} -\frac{\partial^2 \ell}{\partial \alpha^2} &= n\psi_1(\alpha) - n\psi_1\left(\alpha + \frac{k-1}{2}\right) - \frac{n}{\alpha} + \sum_{i=1}^n \frac{2\theta s_i^l + \alpha - (k-1)/2}{(\theta s_i^l + \alpha)^2} \\ -\frac{\partial^2 \ell}{\partial \theta^2} &= -\frac{n\alpha}{\theta^2} + \frac{\alpha}{\theta^2} \left(\alpha + \frac{k-1}{2}\right) \sum_{i=1}^n \frac{2\theta s_i^l + \alpha}{(\theta s_i^l + \alpha)^2} \\ -\frac{\partial^2 \ell}{\partial \theta \partial \alpha} &= \frac{n}{\theta} - \frac{1}{\theta} \sum_{i=1}^n \frac{\alpha^2 + 2\alpha\theta s_i^l + \frac{k-1}{2}\theta s_i^l}{(\theta s_i^l + \alpha)^2}. \end{aligned}$$

where ψ_1 is the trigamma function.

Let $(\hat{\alpha}^l, \hat{\beta}^l)$ be the maximum partial likelihood estimators. Conditioned on (τ_i^l) we have

$$\begin{aligned} \bar{y}_{i+} &\sim \mathcal{N}\left(m_M, \sigma_M^2 + \frac{1}{4k} \left(\frac{1}{\tau_i^1} + \frac{1}{\tau_i^2}\right)\right), \\ \bar{y}_{i-} &\sim \mathcal{N}\left(m_\Delta, \sigma_\Delta^2 + \frac{1}{4k} \left(\frac{1}{\tau_i^1} + \frac{1}{\tau_i^2}\right)\right). \end{aligned}$$

We would then have MLEs

$$\begin{aligned} \hat{m}_M &= \frac{1}{n} \sum_{i=1}^n \bar{y}_{i+}, \\ \hat{m}_\Delta &= \frac{1}{n} \sum_{i=1}^n \bar{y}_{i-}, \end{aligned}$$

which are approximately normally distributed, with means m_M and m_Δ respectively, and conditional on τ_i^l standard errors

$$\frac{\sigma_M^2}{n} + \frac{1}{4kn^2} \sum_{i=1}^n (\tau_i^1)^{-1} + (\tau_i^2)^{-1} \quad \text{and} \quad \frac{\sigma_\Delta^2}{n} + \frac{1}{4kn^2} \sum_{i=1}^n (\tau_i^1)^{-1} + (\tau_i^2)^{-1},$$

which we may approximate — with error on the order of $n^{-3/2}$ — replacing the mean of $(\tau_i^l)^{-1}$ by its expected value $\beta^l/(\alpha^l - 1)$ to obtain

$$\begin{aligned} \text{Var}(\hat{m}_M) &\approx \frac{\sigma_M^2}{n} + \frac{1}{4kn} \left(\frac{\beta^1}{\alpha^1 - 1} + \frac{\beta^2}{\alpha^2 - 1} \right) \\ \text{Var}(\hat{m}_\Delta) &\approx \frac{\sigma_\Delta^2}{n} + \frac{1}{4kn} \left(\frac{\beta^1}{\alpha^1 - 1} + \frac{\beta^2}{\alpha^2 - 1} \right) \end{aligned}$$

Finally, conditioned on the τ_i^l we have that the random variables \bar{y}_{i+} are normal with variance

$$\sigma_M^2 + \frac{1}{4k} \left((\tau_i^1)^{-1} + (\tau_i^2)^{-1} \right),$$

so the unconditional variance is the expected value, or

$$\sigma_M^2 + \frac{1}{4k} \left(\frac{\beta^1}{\alpha^1 - 1} + \frac{\beta^2}{\alpha^2 - 1} \right).$$

This yields the estimators

$$\begin{aligned}\hat{\sigma}_M^2 &= \frac{1}{n-1} \sum_{i=1}^n \left(\bar{y}_{i+} - n^{-1} \sum_{i=1}^n y_{i+} \right)^2 - \frac{1}{4k} \left(\frac{\hat{\beta}^1}{\hat{\alpha}^1 - 1} + \frac{\hat{\beta}^2}{\hat{\alpha}^2 - 1} \right), \\ \hat{\sigma}_\Delta^2 &= \frac{1}{n-1} \sum_{i=1}^n \left(\bar{y}_{i-} - n^{-1} \sum_{i=1}^n y_{i-} \right)^2 - \frac{1}{4k} \left(\frac{\hat{\beta}^1}{\hat{\alpha}^1 - 1} + \frac{\hat{\beta}^2}{\hat{\alpha}^2 - 1} \right).\end{aligned}$$

Using the delta method, and the fact that we see that the variance of $\hat{\beta}/(\hat{\alpha} - 1)$ is approximately

$$\frac{\sigma_\beta^2}{(\hat{\alpha} - 1)^2} + \frac{\hat{\beta}^2 \sigma_\alpha^2}{(\hat{\alpha} - 1)^4},$$

where σ_α and σ_β are the standard errors for $\hat{\alpha}$ and $\hat{\beta}$ respectively, so the standard errors for $\hat{\sigma}_M^2$ and $\hat{\sigma}_\Delta^2$ are approximately

$$\begin{aligned}\text{SE}(\hat{\sigma}_M^2) &\approx \frac{1}{2k} \left(\frac{8k^2 \hat{\sigma}_M^2}{n} + \frac{\sigma_\beta^2}{(\hat{\alpha}^1 - 1)^2} + \frac{(\hat{\beta}^1)^2 \sigma_\alpha^2}{(\hat{\alpha}^1 - 1)^4} + \frac{\sigma_\beta^2}{(\hat{\alpha}^2 - 1)^2} + \frac{(\hat{\beta}^2)^2 \sigma_\alpha^2}{(\hat{\alpha}^2 - 1)^4} \right)^{1/2}, \\ \text{SE}(\hat{\sigma}_\Delta^2) &\approx \frac{1}{2k} \left(\frac{8k^2 \hat{\sigma}_\Delta^2}{n} + \frac{\sigma_\beta^2}{(\hat{\alpha}^1 - 1)^2} + \frac{(\hat{\beta}^1)^2 \sigma_\alpha^2}{(\hat{\alpha}^1 - 1)^4} + \frac{\sigma_\beta^2}{(\hat{\alpha}^2 - 1)^2} + \frac{(\hat{\beta}^2)^2 \sigma_\alpha^2}{(\hat{\alpha}^2 - 1)^4} \right)^{1/2}\end{aligned}$$

Now compute the combined variance

For a parameter like α we estimate the variance of $\hat{\alpha}$ by

$$\text{Var}(\hat{\alpha}) = \mathbb{E}[\text{Var}(\hat{\alpha} | I)] + \text{Var}(\mathbb{E}[\hat{\alpha} | I]).$$

Here I represents the randomly imputed fractional part. We can estimate the first term by averaging the estimated variance (from Fisher Information) over all random imputations. We estimate the second term by the variance of the α estimates over imputations. Note that this is not quite right, since what we really want the variance of is $\alpha_0(I)$ — effectively, the “true” parameter consistent with the imputation. This is a plug-in estimate, as is the Fisher Information estimate of the variance.

Computing residuals

We define the deviance for an individual i with observations (Y_i) given the hyperparameters $h = (m_M, m_\Delta, \sigma_M^2, \sigma_\Delta^2, \alpha^H, \theta^H, \alpha^C, \theta^C)$

$$D = \sum_{i=1}^n \log \mathbb{P}\{\mathbf{Y}_i | \text{hyperparameters} = h\}.$$

Since the \mathbf{Y}_i are independent conditioned on h ,

$$\begin{aligned}D &= \sum_{i=1}^n \log \mathbb{E}_h [\mathbb{P}\{\mathbf{Y}_i | M_i, \Delta_i, \tau_i^C, \tau_i^H\}] \\ &\approx \sum_{i=1}^n \log \frac{1}{R} \sum_{r=1}^R [\mathbb{P}\{\mathbf{Y}_i | M_{i,r}, \Delta_{i,r}, \tau_{i,r}^C, \tau_{i,r}^H\}] \frac{\pi_h(M_{i,r}, \Delta_{i,r}, \tau_{i,r}^C, \tau_{i,r}^H)}{q(M_{i,r}, \Delta_{i,r}, \tau_{i,r}^C, \tau_{i,r}^H | h, \mathbf{Y}_i)},\end{aligned}$$

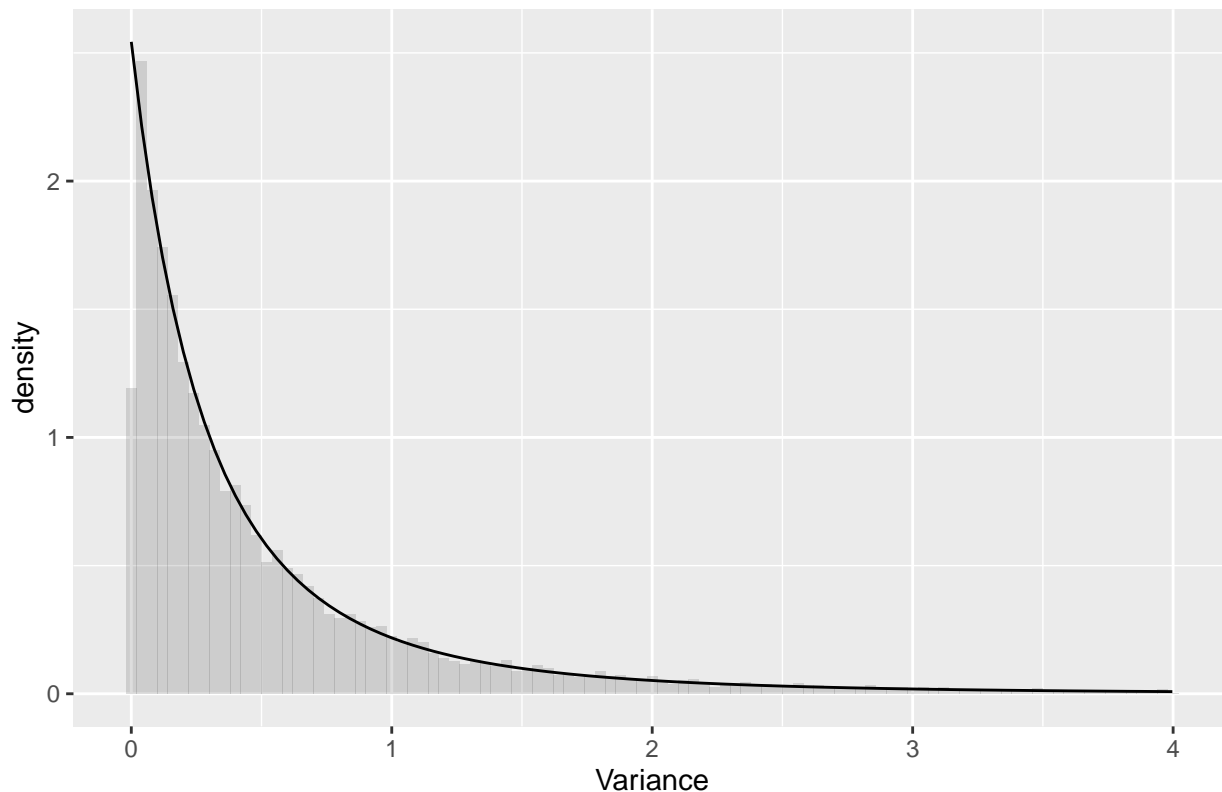
where $(M_{i,r}, \Delta_{i,r}, \tau_{i,r}^C, \tau_{i,r}^H)$ are independent samples from a distribution q that may depend on \mathbf{Y}_i and h , and π_h is the true density of those individual parameters given hyperparameters h .

Check variance distribution empirically

We wish to check whether the continuous distribution we have fit for individual variances describes the true distribution of variances in the population reasonably well. The first thing we do is to compare the empirical variances (with imputed fractional parts) to the theoretical beta-prime distribution. To match the standard distribution, the variances are normalized by being divided by the factor α/θ . Note that the distribution has a very long tail, and we have truncated the plot at a point where about

```
## NULL
```

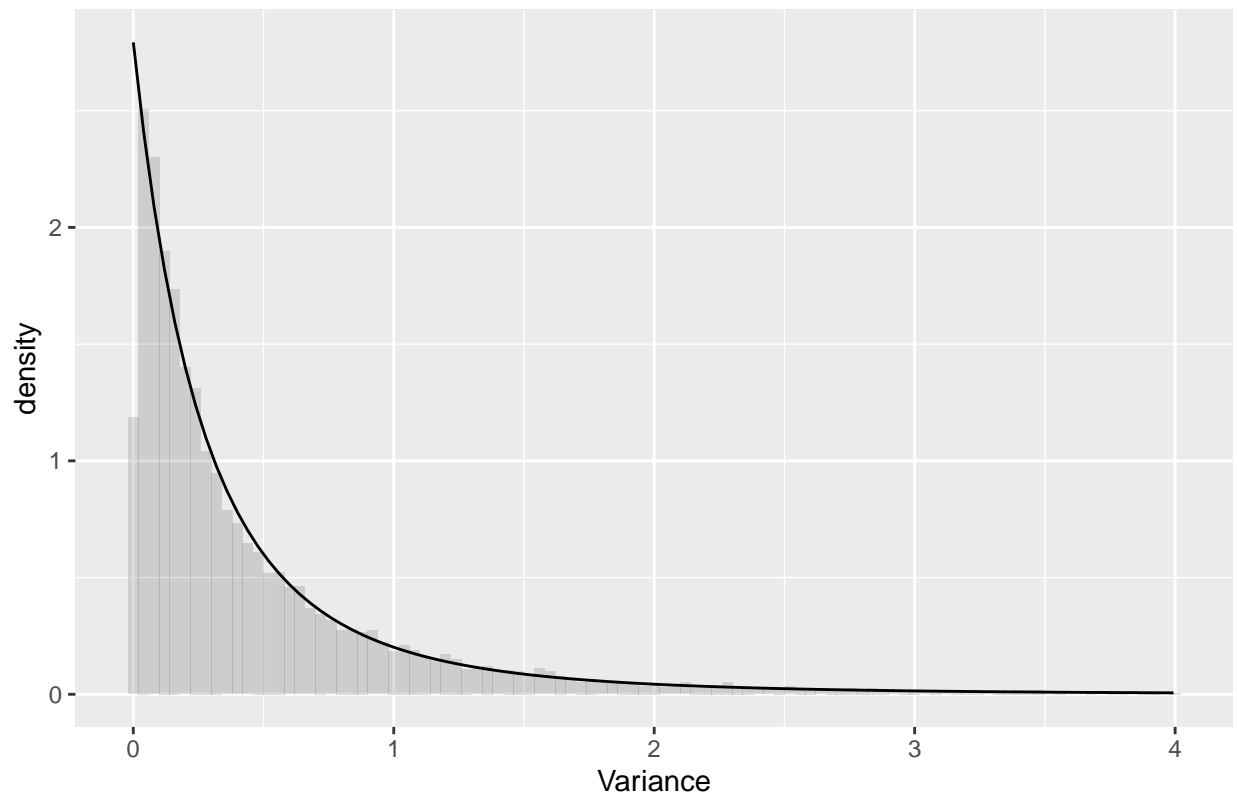
Systolic Clinic : Histogram of Variances/beta



test-1.pdf

```
## NULL
```

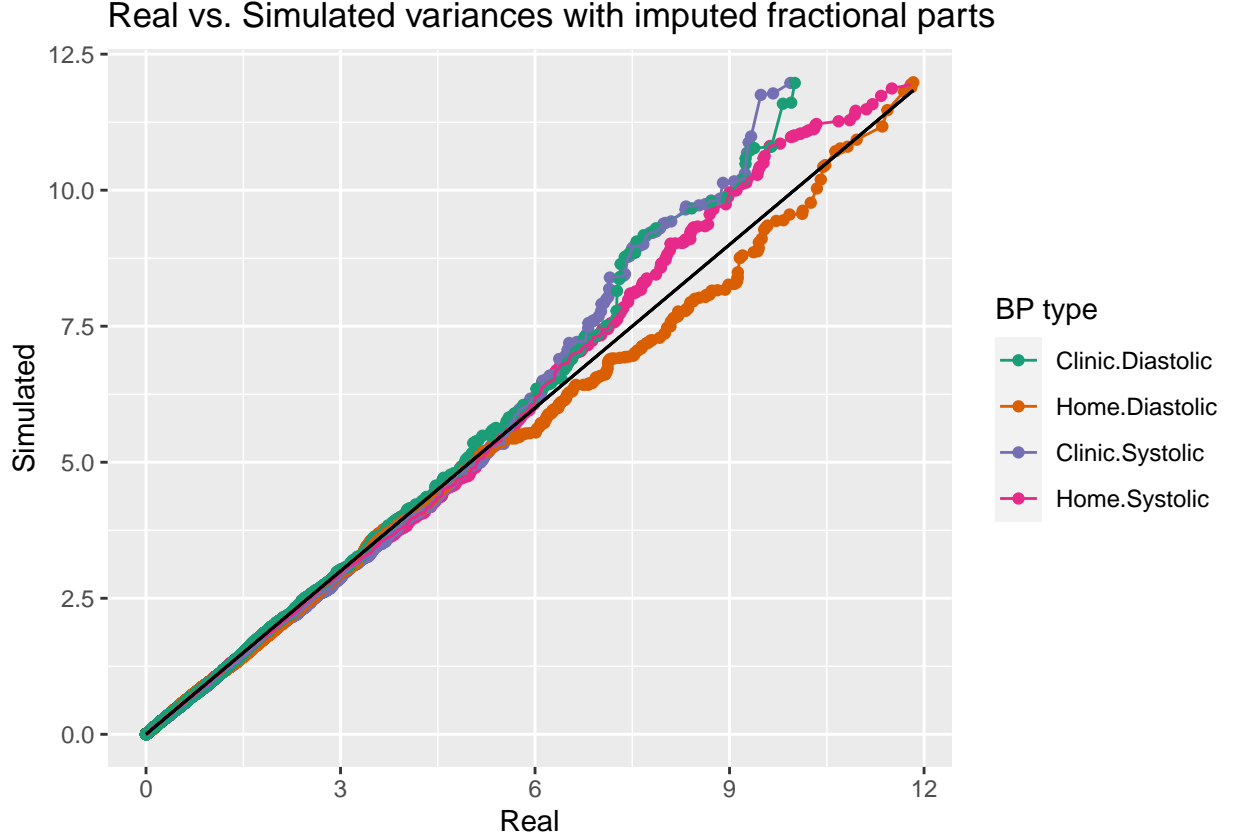
Diastolic Clinic : Histogram of Variances/beta



test-2.pdf

Now we generate data from the inferred model that mimic the true data, with three systolic and three diastolic BP measures per person. These cannot be directly compared with the observed data, which are rounded to the nearest 2 (in a somewhat biased way), so we randomly impute the fractional part, which we add to the true observations. This gives us a set of true variances and a set of simulated variances, which we hope will have approximately the same distribution. We compare these — for each of the four combinations of systolic/diastolic and home/clinic — by Q-Q plots.

```
## Warning: Multiple drawing groups in `geom_function()`. Did you use the correct
## `group`, `colour`, or `fill` aesthetics?
```



variances-1.pdf

Hamiltonian Monte Carlo (HMC)

The model, as described in the article, is a Bayesian hierarchical model. In order to parameterize such an intricate model, traditional Maximum Likelihood Estimation methods can no longer be applied. Therefore, we apply the Hamiltonian Monte Carlo (HMC) method. HMC is a form of Markov Chain Monte Carlo methods, which samples potential parameter space values of the model, then calculates directly the likelihood function based on that choice of parameters. The derivative of the likelihood function, ϕ , guides parameter space exploration in θ towards the modal value of the joint posterior distribution. This method is ideal for complicated, non-Gaussian distribution forms. The three steps of HMC are:

1. Draw a sample of the derivative ϕ using the posterior distribution of ϕ , which is the same as its prior.
2. Update the values of θ^* and ϕ^* using

$$\theta^* \leftarrow \theta + \epsilon M^{-1} \phi, \quad (11)$$

and

$$\phi \leftarrow \phi + \epsilon \frac{1}{2} \frac{d \log \{p(\theta|y)\}}{d\theta}, \quad (12)$$

where M is the jacobian of the parameters. This can be set to a diagonal matrix for no correlation between parameters, and is pointwise updated throughout the calculation. This is the leapfrog method, whereby ϵ dictates the scale size of the step to ensure convergence on the correct point is made, and L is the number of steps to be ‘leaped’.

3. Compute the rejection parameter:

$$r = \frac{p(\theta^*|y)p(\phi^*)}{p(\theta^{t-1}|y)p(\phi^{t-1})} \quad (13)$$

4. Set θ^t to θ^* with probability $\min\{1, r\}$, or otherwise keep θ^{t-1} .

The tuning parameters ϵ and L should be chosen according to a desired acceptance rate. The No-U-Turn Sampler of Stan automates the calculation of these tuning parameters. A more detailed overview of HMC and the NUTS algorithm integrated into the Stan package, see ‘*The No-U-Turn Sampler: Adaptively Setting Path Lengths in Hamiltonian Monte Carlo*’ by M. Hoffman and A. Gelman, Journal of Machine Learning Research, 15, 1351-1381 (2014).

Centering the Linear Predictor

During the MCMC simulations, the centering values play a non-negligible role in shaping the model parameterization. If the centering parameters are held constant throughout all of the MCMC simulations, then the equation $\sum_i^N \exp(\beta \cdot (\mathbf{X} - \hat{\mathbf{X}})) = 0$ is no longer guaranteed. However, automatically defining the centering values based on the model parameters sampled at the current MCMC iteration is not advisable as it can lead to poor parameter convergence. This is because it modifies the likelihood function at every MCMC iteration. Therefore, we iterate the MCMC algorithm multiple times. At every iteration, we recalculate the centering parameters to satisfy the requirement that the average of the linear predictor term going to zero, based on the posterior distributions of the previous MCMC simulation. This iteration is carried out until the centering parameters converge. Convergence is defined by optimising on two factors. The first is that the sum of the linear predictor term across all MCMC samples needs to tend to negligible values (we define this as the average difference being less than 10^{-7}), see figure 3. The second convergence criteria is that the average Root Mean-Squared Error (RMSE) of the model predictions on the survival outcomes in the MCMC simulations needs to also decrease towards zero, see figure 3 (top). For the second criteria, we stopped the simulations when either the difference in the RMSE stopped decreasing (below a threshold of 1%), or the RMSE value was less than 20, see figure 3 (bottom). Illustration of the convergence is shown in figure 3.

Code Description

The code can be found at <https://github.com/hamishwp/Nhanes2021>. The numerical code has been built in multiple stages. Below, we explain the principal files required to replicate the entire analysis presented in the article. There are 5 main groups for the code:

1. Data cleaning scripts
2. Main file
3. Stan files for HMC
4. Centering recalculation scripts
5. Post-processing analysis

We provide a brief description of each of these below.

Data Cleaning

This is found in the file `Dataclean2021.R`. Provided the raw NHANES dataset (in CSV format), it extracts all the data required for the simulations, and stores it in a structure that can be directly read in to the main file (`MCMC_DiasSyst_v3.R`) of this research.

Main

The main file is `MCMC_DiasSyst_v3.R`. It reads in the cleaned NHANES data, the specific choice of simulation parameters (for example, whether to use the FRS number or mean systolic & diastolic blood pressure), and runs the correct RStan scripts for that specific selection of simulation parameters. This script is intended for use on computing clusters.

Stan

There are eight Stan files:

1. `mystanmodel_DS_sigma_v2_autopred.stan`
2. `mystanmodel_DS_tau_v2_autopred.stan`
3. `mystanmodelFRS_DS_sigma_v2_autopred.stan`
4. `mystanmodelFRS_DS_tau_v2_autopred.stan`
5. `mystanmodel_DS_sigma_v2.stan`
6. `mystanmodel_DS_tau_v2.stan`
7. `mystanmodelFRS_DS_sigma_v2.stan`
8. `mystanmodelFRS_DS_tau_v2.stan`

These correspond to the following alternative simulation parameters:

- For the blood-pressure variability, choosing to use the standard-deviation σ or the precision $\tau = 1/\sigma$
- Using the FRS score or the mean diastolic and systolic blood pressure as a covariate in the analysis
- Whether the centering parameters, \hat{X} , in the linear predictor term are automatically calculated to satisfy $\sum_i^N \exp(\beta \cdot (\mathbf{X} - \hat{X})) = 0$ for every MCMC iteration, or whether the centering is held constant across all iterations

Centering

The centering of the linear predictors, which is required as input to every MCMC simulation iteration, is recalculated in the files `AutoPred_Recalc.R` and `ManPred_Recalc.R`. This is then provided to the Main script, `MCMC_DiasSyst_v3.R`, which provides these centering values to the Stan code for the MCMC simulations.

Empirical Bayes Estimation

The file `gamma_fits.Rmd` contains all the necessary routines in order to replicate the calculation of the empirical Bayes' priors for the hyperparameters of the model.

####Post-processing The post-processing script is called `PostProcessing.R`, which heavily relies on the `Functions.R` script which contains all the necessary functions to analyse the data. The post-processing script generates many useful plots of the MCMC posterior distribution for the user, including Bayes' factors, violin plots of the normalised beta and gompertz posteriors, and more.

Results

In this section, we add some additional detail to the results section covered in the article. Extra information is given to explain how convergence of the simulations was ensured, and to also include more visualisations of the converged model parameterizations. The authors feel that this is particularly useful to provide confidence in the model parameterization and the predictions.

Convergence of Simulations

Convergence of the simulations required to parameterize the model presented in this work is required for the MCMC simulations performed by Stan, as well as convergence in the centering values that requires repeating the Stan calculations several times. Convergence of the latter is shown in figure 3. The upper plot in figure 3 illustrates convergence in the average Root Mean-Squared Error (RMSE) of the model predictions on the survival outcomes in the MCMC simulations. The lower plot in figure 3 illustrates convergence in the average sum of the linear predictor terms over all MCMC chain iterations.

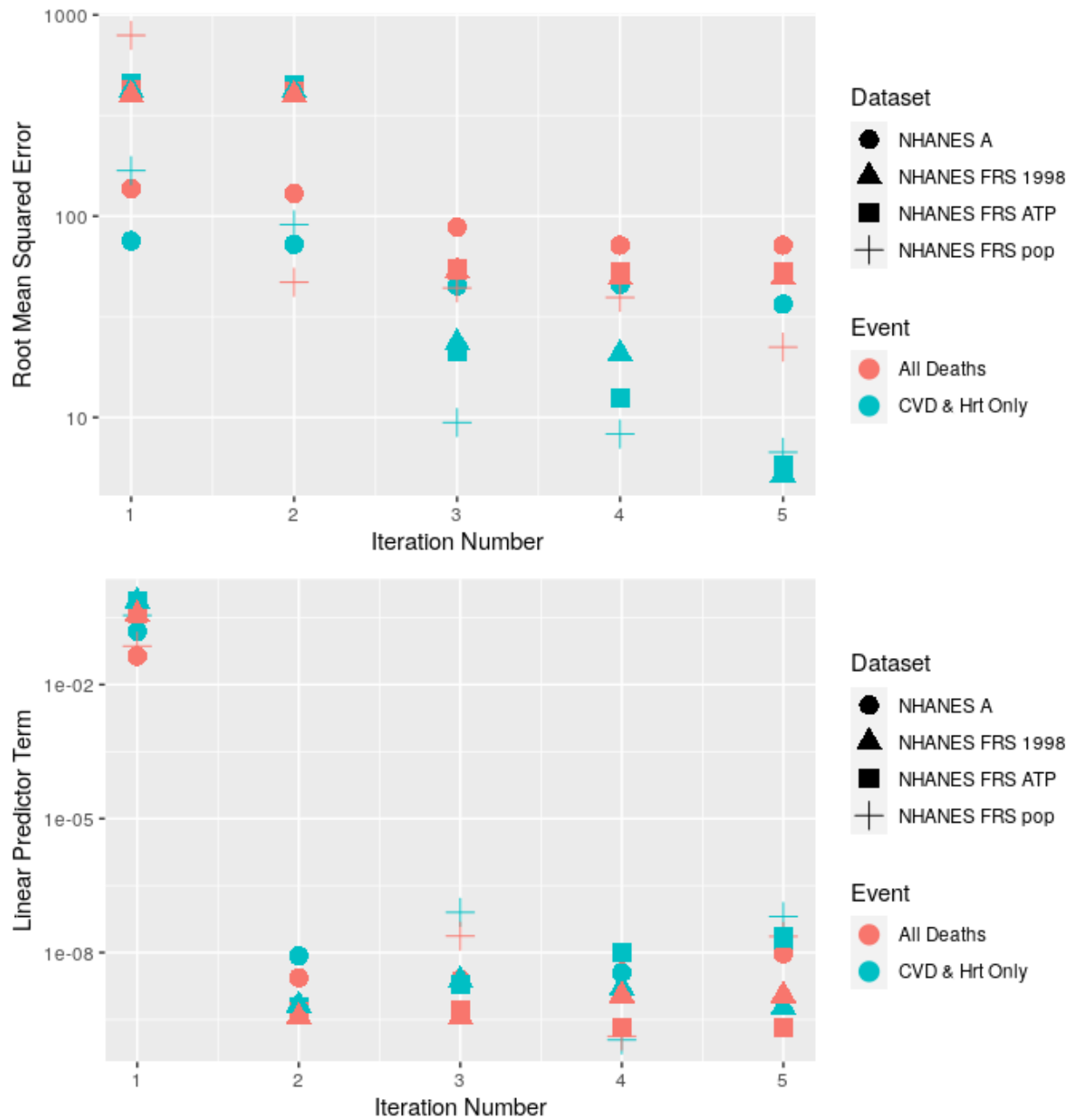


Figure 3: Illustration of the convergence of the centering parameters of the model.

With respect to convergence of the MCMC simulations, defining convergence first involves discarding the burn-in period of the simulations. When the time-evolution marker chain has a large number of samples, sequence thinning is used to reduce the amount of data storage - after convergence, take only the k th value of the simulations (after having discarded the burn-in phase values) and discard the rest. One measure of convergence is to bin similar markers and check that for each bin, the variation of the individual marker movement over a few time steps is larger than the variation of the ensemble markers in-between one-another. Other methods of convergence are stationarity and mixing. The former occurs by ensuring that the gradients of movements in the chains in time are in the same direction, the latter ensures that the amplitude of the movements in the chains are similar. To calculate the mixing and stationarity, one can do the following:

- Take the proposedly converged marker population, where there are N markers in total each of index length τ (thus of total physical time quantity $t\tau$). Split it k times, where k is a common denominator of τ .
- Now you have kN MCMC chains each of length $|\tau/k|$
- For the marker ψ_{ij} with i and j the chain length (time) and marker number indices respectively, then the mean marker value over the chain length (time) is

$$\bar{\psi}_{|j} = \frac{k}{\tau} \sum_{i=1}^{\tau/k} \psi_{ij} \quad (14)$$

and the total average quantity of ψ over all markers, over all chain lengths is therefore

$$\bar{\psi}_{||} = \frac{1}{kN} \sum_{j=1}^{kN} \bar{\psi}_{|j} \quad (15)$$

- Stationarity: compare the inter-marker variance (between sequence B):

$$B = \frac{\tau}{k(kN-1)} \sum_{j=1}^{kN} (\bar{\psi}_{|j} - \bar{\psi}_{||})^2 \quad (16)$$

- Mixing: compare the variance along each markers chain length (within-sequence W):

$$W = \frac{1}{n(\tau-k)} \sum_{j=1}^{kN} \sum_{i=1}^{\tau/k} (\psi_{i,j} - \bar{\psi}_{|j})^2 \quad (17)$$

- Therefore, to estimate the marginal posterior variance of $p(\psi|y)$, then we use a weighted average

$$\hat{\text{Var}}^+(\psi|y) = \frac{\tau-k}{N} W + \frac{1}{Nk} B \quad (18)$$

Note that this quantity overestimates the marginal posterior variance, but it is unbiased under stationarity: this can be used to infer convergence. When the variation in

$$\hat{R} = \sqrt{\frac{\hat{\text{Var}}^+(\psi|y)}{W}} \quad (19)$$

should approach close to 1 for converged simulations.

Another convergence parameter is the number of effective independent marker draws. Upon convergence, the time evolution of each marker should be uncorrelated and independent to previous time steps. To find the average time-correlation over all particles, we use the variogram V_t :

$$V_t = \frac{1}{Nk(\tau/k - \bar{t})} \sum_{j=1}^{kN} \sum_{i=1}^{\tau/k} (\psi_{i,j} - \psi_{i-\bar{t},j})^2, \quad (20)$$

where $\tilde{t} \in 1, 2, \dots, \tau/k$ is a time index. Then we get the time-correlations:

$$\hat{\rho}_t = 1 - \frac{V_t}{2\hat{\text{Var}}_+} \quad (21)$$

This comes from the expectation of the variance $E[(\psi_i - \psi_{i-t})^2] = 2(1 - \rho_t)\text{Var}(\psi)$. This can be used to infer the effective number of independent marker draws:

$$\hat{n}_{eff} = \frac{mn}{1 + 2 \sum_{\tilde{t}=1}^T \hat{\rho}_{\tilde{t}}} \quad (22)$$

Where T is the index at which the sum of the autocorrelation estimates $\hat{\rho}_{t'} + \hat{\rho}_{t'+1}$ is negative. As a general guide, we should have $\hat{n}_{eff} \sim 10N/k$ effective independent marker draws and that $\hat{R} \rightarrow 1 \sim 1.1$. In this research, we continued running the MCMC simulations until these two criteria were met (and went beyond: $\hat{R} < 1.05$ for all parameters in all models and that $\hat{n}_{eff} > 750$ for all parameters in all models).

Results - Model Parameterization

We remind the reader of the list of numbers of the different models explored in this research, provided in the list found in section ‘Proposed Models’. The authors will use the numbers in the list, referred to as the run number, in the following plots. One of the most important set of parameters of the model is the vector β of covariates in the Cox’ proportional hazards model. When the β vector is normalised, the larger (in absolute terms) the value of β , the larger the correlation between that specific covariate and the risk of mortality. Positive values of β imply a higher risk of mortality, and the inverse for negative values of β . As we can see from the violin plots of the MCMC posterior samples of the β parameters in figure 4, the parameter that correlated the highest with both the mortality risk of CVD and for all mortalities, in absolute terms, was the 1998 version of the FRS score, shown in the top-right plot under run numbers 7 and 8. The FRS-1998 score correlated, on average over all the MCMC iterations, approximately 25% more with mortality risk of CVD than the (more recently developed) FRS ATP III score. A similar, but slightly weaker, correlation was found between the two FSR scores for all mortality-based risk. The middle-left plot in figure 4 shows that the mean diastolic blood pressure acts to decrease mortality risk. Finally, the influence of the longer-term difference in the mean blood pressure, displayed in the top-left and top-middle plots of figure 4, is also shown to increase mortality risk across all run numbers. The influence of the blood-pressure variability on mortality is illustrated to not be consistent across simulations, whereby the statistical significance of the effect is lower than for the other parameters in the linear predictor term.

With respect to the time-independent Gompertz parameter, described using B in this article, the results between all models that simulate CVD mortality risk, and all the models that simulation all-cause mortality risk are consistent with one-another. This is illustrated by the similarity between plots on the left hand side and the right hand side of figure 5. The consistency appears across sex assigned at birth and race.

Figure 6 reflects the same level of consistency for the Gompertz parameter that influences the temporal evolution of the mortality risk. It is worth noting that both figures 5 and 6 have inverse trends between the values of B and θ for each demographic group. This makes it difficult to imagine, based on these two plots, what the mortality risk is at different ages across demographics, yet it is evident that the form of the change in the mortality risk curve in time is different for each demographic group. Women are observed to have lower initial values of risk, but mortality risk later in life begins to increase much faster than for men. Additionally, hispanic populations are shown to have a larger initial mortality risk than black populations who are shown to have a larger initial mortality risk than white populations in the USA. However, mortality risk increases at a faster rate for white populations than for black populations, for which it increases faster than hispanic populations in the USA.

To measure the performance of the model to predict the survival outcome of individuals in the population, figure 7 shows, ordered by individual age, the cumulative hazard $H(t)$ predicted against the cumulative number of deaths in the populations, for each model explored in this research. Each model is shown to predict survival outcomes reliably, across the entire age range of the population.

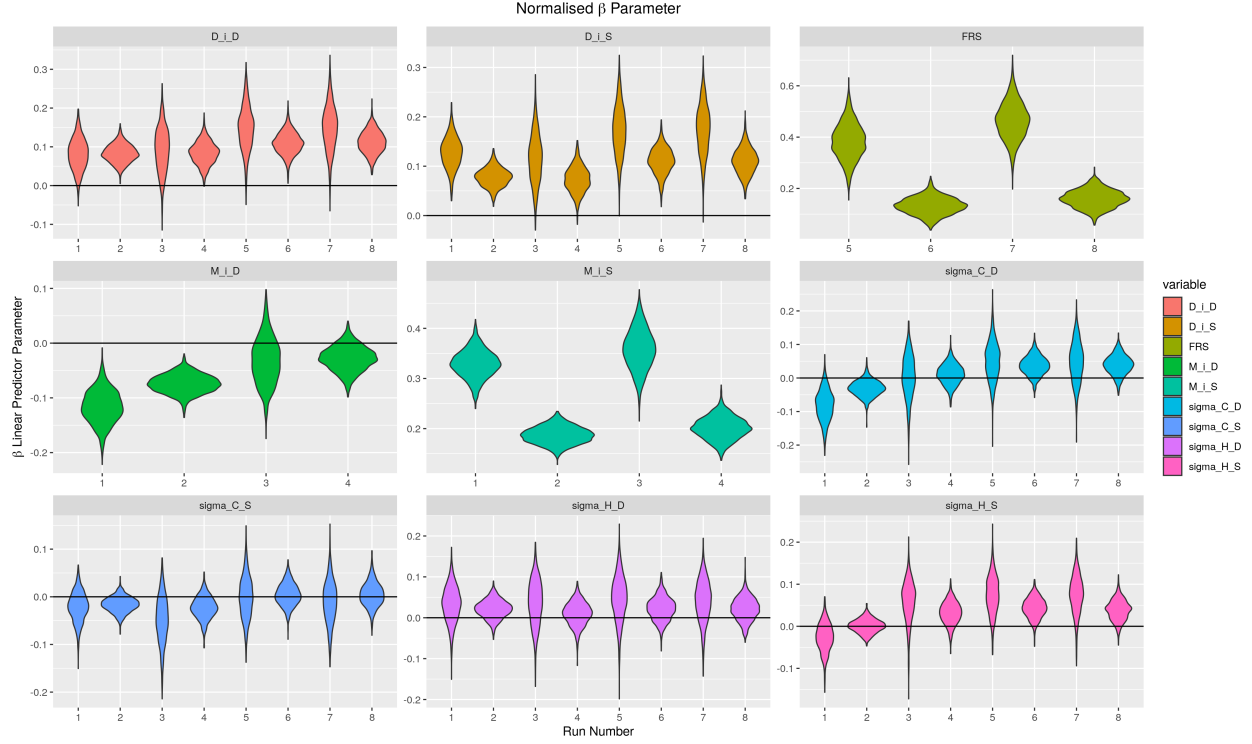


Figure 4: Violin plots of the normalised β parameters of the different models.

The concordance index is an instrument for quantifying the accuracy of risk scores to predict survival outcomes between many individuals in a given population. The best advantage of the concordance index is for survey or census data that includes censoring. To see the exact method for the concordance index presented below, including the confidence intervals, please see M. J. Pencina and R.B D’Agostino (2004). The concordance index compares all individuals who had a death outcome with all other individuals who either died or were censored at a later age than the first individual. For each pair the risk scores (in this work, this is the relative risk, h) are compared, and the accuracy of the model is thereby reflected by having individuals with lower risk scores outliving the other individual. For two individuals, a and b , whereby individual a had a death at time T_a and individual b had either a death or was censored at time T_b , they are both said to be concordant if $h_a > h_b$ and $T_a < T_b$, and discordant if $h_a < h_b$ and $T_a < T_b$. By evaluating this over the entire population, this provides an estimation of the accuracy of using the risk score to predict survival outcomes in the population. Table @ref(tab:concord_var) provides the concordance indices and their $\alpha = 0.05$ confidence intervals for each of the different runs (that correspond to table @ref(tab:runnumbers)), for a variety of different models.

Model	Run Number 1	Run Number 2	Run Number 3
Full model	0.564 (0.517-0.61)	0.51 (0.487-0.533)	0.624 (0.567-0.678)
FRS or mean systolic BP	0.57 (0.523-0.615)	0.516 (0.492-0.539)	0.618 (0.561-0.672)
FRS or mean systolic & diastolic BP	0.552 (0.505-0.597)	0.505 (0.482-0.529)	0.618 (0.561-0.672)
No short-term variation (sigmas)	0.558 (0.511-0.603)	0.507 (0.484-0.53)	0.618 (0.561-0.672)
Gompertz only	0.553 (0.507-0.599)	0.54 (0.516-0.563)	0.59 (0.532-0.644)
No time or age dependency	0.627 (0.581-0.671)	0.599 (0.576-0.621)	0.642 (0.585-0.695)

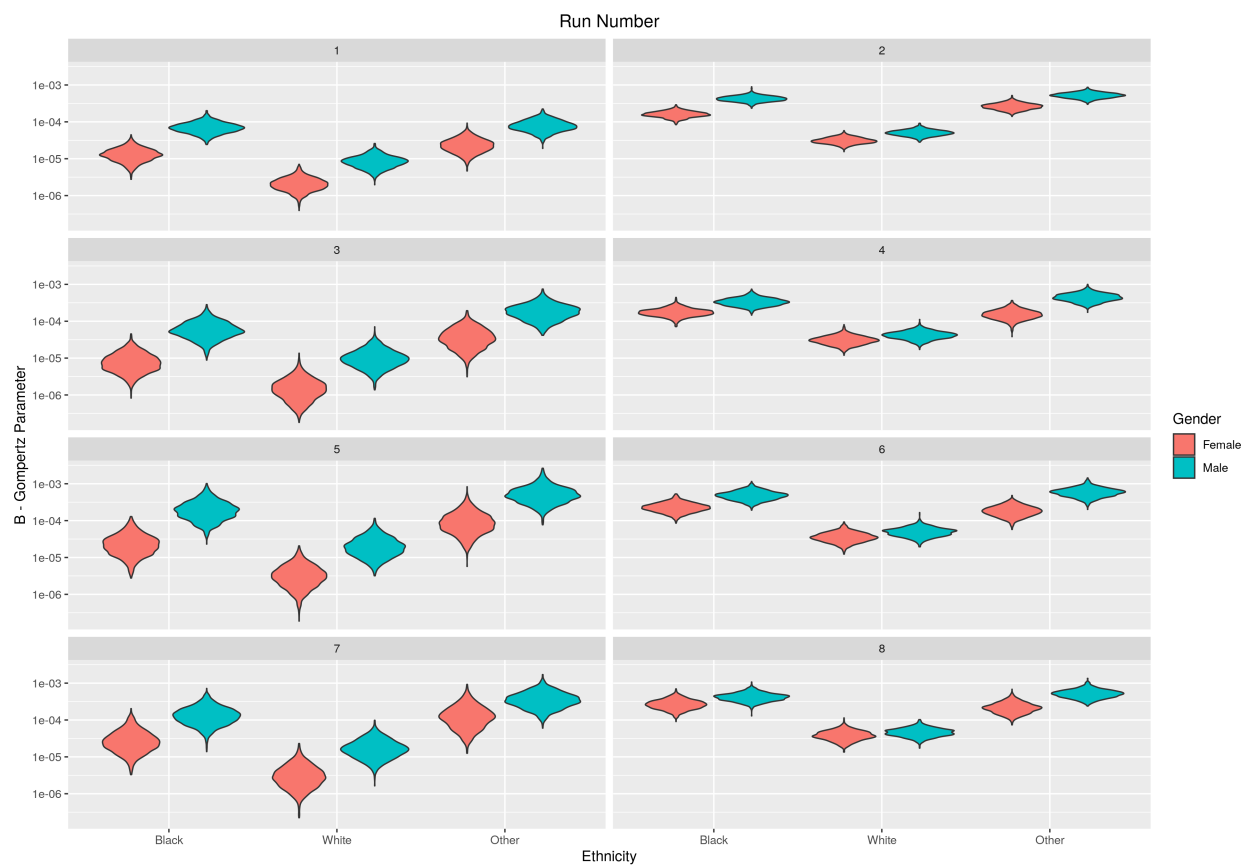


Figure 5: Violin plots of the normalised B parameter (from the Gompertz equation) of the different models.

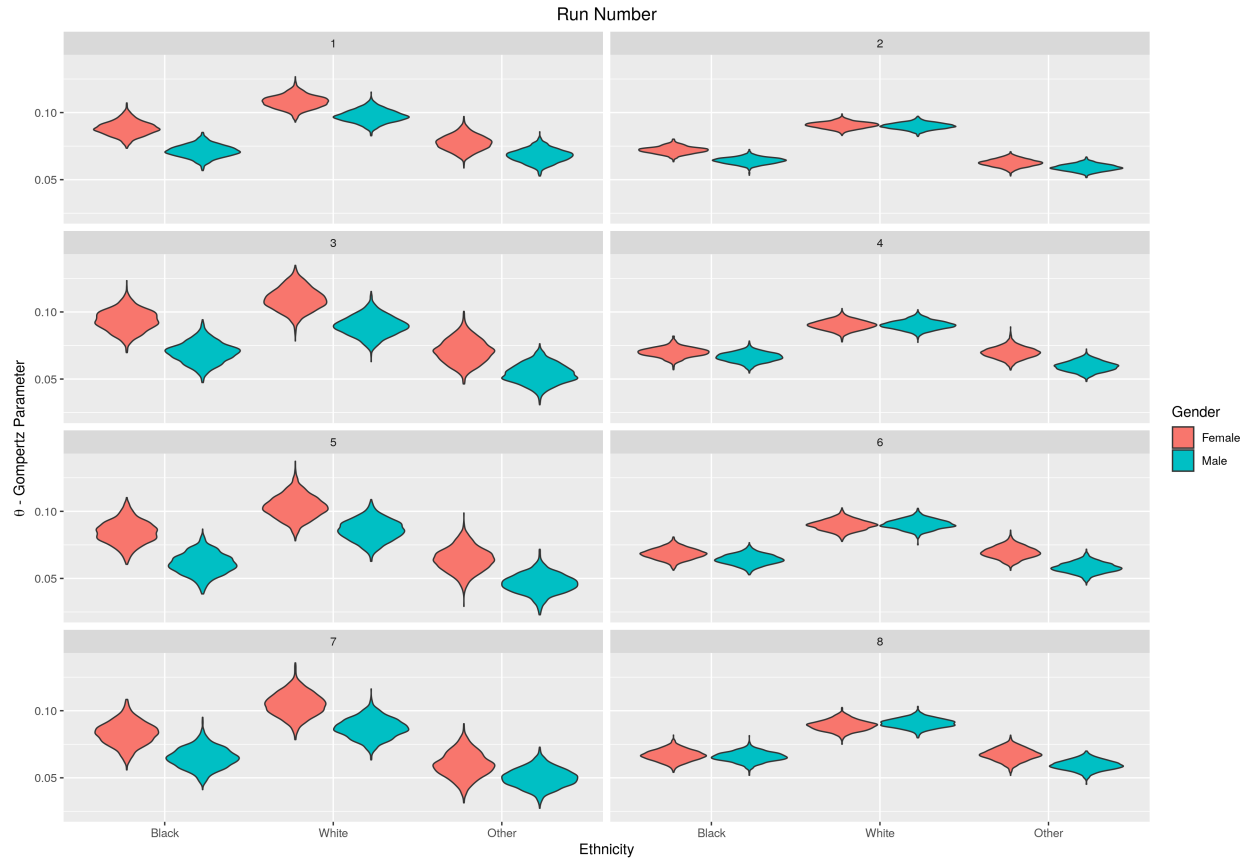


Figure 6: Violin plots of the normalised θ parameter (from the Gompertz equation) of the different models.

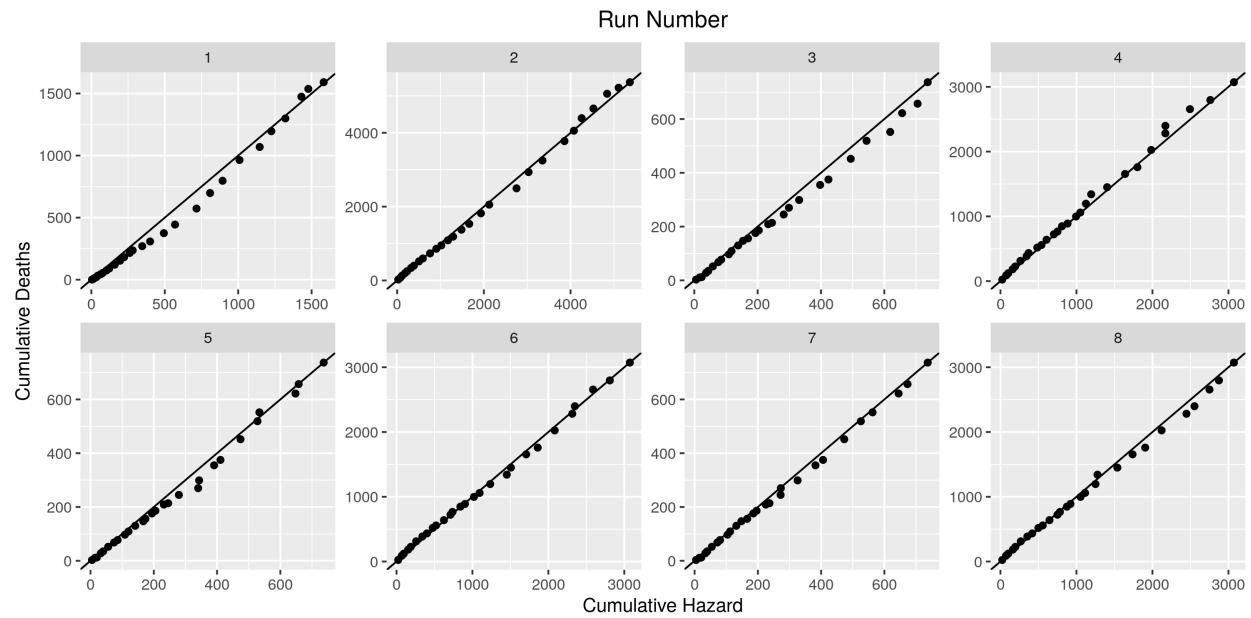


Figure 7: Predicted cumulative hazard against cumulative number of deaths in the population, ordered by the age of the individual.

Model	Run Number 4	Run Number 5	Run Number 6
Full model	0.555 (0.528-0.582)	0.555 (0.498-0.611)	0.528 (0.501-0.555)
FRS or mean systolic BP	0.551 (0.524-0.578)	0.522 (0.464-0.578)	0.513 (0.486-0.54)
FRS or mean systolic & diastolic BP	0.551 (0.524-0.578)	0.522 (0.464-0.578)	0.513 (0.486-0.54)
No short-term variation (sigmas)	0.55 (0.522-0.576)	0.543 (0.486-0.6)	0.523 (0.496-0.55)
Gompertz only	0.558 (0.531-0.585)	0.607 (0.55-0.662)	0.564 (0.537-0.591)
No time or age dependency	0.59 (0.563-0.617)	0.624 (0.567-0.678)	0.58 (0.553-0.606)

Model	Run Number 7	Run Number 8
Full model	0.578 (0.521-0.634)	0.535 (0.508-0.562)
FRS or mean systolic BP	0.545 (0.487-0.601)	0.521 (0.494-0.548)
FRS or mean systolic & diastolic BP	0.545 (0.487-0.601)	0.521 (0.494-0.548)
No short-term variation (sigmas)	0.567 (0.51-0.623)	0.53 (0.503-0.557)
Gompertz only	0.601 (0.543-0.655)	0.563 (0.535-0.589)
No time or age dependency	0.627 (0.57-0.68)	0.58 (0.553-0.607)

The results show that models that do not include time-at-outcome information (by setting the Gompertz parameter, θ , to zero), but still include blood pressure covariates are stronger predictors of mortality risk, as compared to the full model. We find, as expected, that models trained specifically on CVD and heart-attack related mortality to be more accurate than trained on all mortality events. Additionally, there does not appear to be a statistically significant advantage of using either of the FRS covariates instead of the mean systolic and diastolic blood pressure to predict survival outcomes. By calculating the concordance index for specific demographic groups, we can also evaluate the performance of the full models per group, as shown in table @ref(tab:concord_demo). The results indicate that the performance of the predictions do vary between demographic groups. For CVD and heart-attack mortality, the average concordance index for the black female population was 0.58, black male population 0.52, other female population 0.53, other male population 0.47, white female population 0.55 and white male population 0.57. Therefore, the accuracy of this model is visibly less accurate for the non-black or white ethnic populations in the survey. On average across CVD and heart attack mortality, the models were more accurate for the female population (0.56) than the male population (0.53).

Model	Run Number 1	Run Number 2	Run Number 3	Run Number 4
Black & female	0.568 (0.423-0.703)	0.492 (0.425-0.56)	0.659 (0.492-0.794)	0.546 (0.473-0.616)
Black & male	0.542 (0.422-0.657)	0.476 (0.417-0.535)	0.572 (0.434-0.7)	0.521 (0.457-0.585)
Other & female	0.532 (0.366-0.691)	0.467 (0.392-0.542)	0.549 (0.389-0.699)	0.489 (0.41-0.569)
Other & male	0.533 (0.409-0.653)	0.481 (0.421-0.542)	0.548 (0.421-0.668)	0.511 (0.443-0.579)
White & female	0.543 (0.45-0.632)	0.45 (0.404-0.498)	0.591 (0.45-0.719)	0.494 (0.433-0.555)
White & male	0.539 (0.459-0.617)	0.465 (0.422-0.508)	0.6 (0.477-0.712)	0.504 (0.447-0.562)

Model	Run Number 5	Run Number 6	Run Number 7	Run Number 8
Black & female	0.555 (0.392-0.707)	0.502 (0.43-0.574)	0.586 (0.421-0.734)	0.499 (0.428-0.571)
Black & male	0.48 (0.348-0.616)	0.459 (0.395-0.523)	0.507 (0.372-0.641)	0.472 (0.408-0.536)
Other & female	0.545 (0.385-0.696)	0.482 (0.403-0.562)	0.525 (0.367-0.679)	0.468 (0.389-0.548)
Other & male	0.395 (0.28-0.523)	0.434 (0.368-0.503)	0.425 (0.307-0.553)	0.452 (0.385-0.52)
White & female	0.535 (0.396-0.669)	0.468 (0.408-0.53)	0.553 (0.413-0.685)	0.477 (0.417-0.539)
White & male	0.584 (0.461-0.697)	0.479 (0.422-0.537)	0.59 (0.467-0.702)	0.485 (0.428-0.543)

An alternative to the concordance index is the dynamic AUC for the binary classification into Died or Survived for death at a particular age (or age range), among the population still alive at the beginning of the age range. As discussed in [Heagerty, P. J., & Zheng, Y. (2005). Survival model predictive accuracy and ROC curves. *Biometrics*, 61(1), 92-105], the concordance may be understood as a weighted average over all times

of the dynamic AUC. The results, per run number, are illustrated in figure 8. We expect the model to lose discriminatory power the further the time of BP ascertainment recedes into the past, and this is reflected in the AUC declining toward 0.5 at more advanced ages.

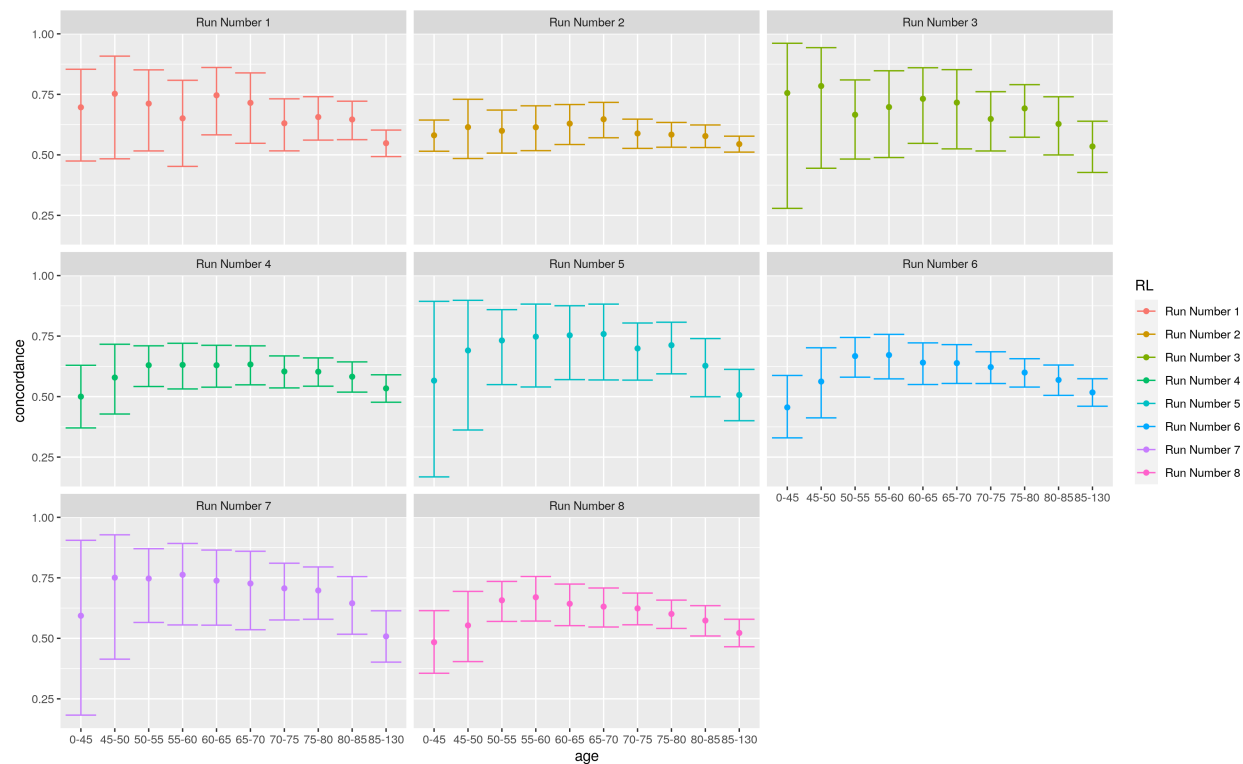


Figure 8: Time-dependent concordance index (AUC), per run number.